

EFFECT OF AIR-FLOW PARAMETERS ON THE MORPHOLOGY OF NANOFIBROUS YARNS BY BLOWN BUBBLE-SPINNING

by

**Hao DOU^{a*}, Shao-Wen YAO^{b*}, Xue MENG^a, Wei FAN^a,
Yun-Yu LI^a, and Hong-Yan LIU^c**

^a School of Textile Science and Engineering, Xi'an Polytechnic University,
Xi'an, Shaanxi Province, China

^b School of Mathematics and Information Science, Henan Polytechnic University, Jiaozuo, China

^c School of Fashion Technology, Zhongyuan University of Technology, Zhengzhou, China

Original scientific paper

<https://doi.org/10.2298/TSCI2004637D>

Blown bubble-spinning was recently explored for the effective fabrication of nanofibrous yarns in a one-step process. In this study, air-flow's temperature and velocity, which play the key role in the formation and morphology of nanofibers, are investigated and optimized. The present study offers a beneficial opportunity for the scale-up production of nanofibrous yarns in the future.

Key words: *thermodynamic, nanofibrous yarns, air-flow, bubble spinning*

Introduction

Nanofibers, which naturally own specific properties such as tiny diameter, high geometric potential (surface energy), and small pore size with high porosity, have been widely used in lots of fields [1, 2], and much attention has been paid to the fabrication of various structured nanofibers with multi-functions for further applications. Liu and He [3] fabricated the PVDF/Fe₂O₃/Zn(Ac)₂ nanofibers using bubble-electrospinning as well as theoretically and experimentally investigated the wettability of nanomaterials with a new concept of the geometric potential theory. Based on the laminar flow theory, Tian *et al.* [4] achieved the self-assembly of PVA macromolecules via adjusting the length and diameter of carbon nanotubes used in electrospinning. Moreover, the mechanical property of nanofibrous membranes was greatly improved by controlling the macromolecule orientation, which resulted from biomimicking the hierarchy of natural spider silks [5]. As one special kind of nanofibers, nanofibrous yarns, which structurally resemble the hierarchical architecture of natural fibers, will increase the entanglement of nanofibers by inserting twist, and enhance the mechanical properties via integration of various structures, leading to potential applications on reinforced composite, artificial ligament and smart wearable clothing, *etc.*

It is notable that electrospinning, as a simple and versatile method [6], has shown huge potential to produce nanofibrous yarns by using a special electrospinning setup consisting of two oppositely charged nozzles [7] or a dynamic liquid vortex system [8] or other auxiliary approaches [9]. However, current challenges like clogging needles, low production and high voltages hazard in operation are still not effectively solved [10]. Therefore, it is critical to develop simple, low-cost, and scalable methods on the basis of the existing nanospinning technologies.

* Corresponding author, e-mail: ysw140917@163.com; douhaosuda@126.com

Recently, the blown bubble spinning, which was derived from the highly commercialized melt blowing process and bubble-electrospinning, has been demonstrated as a novel one-step process for producing nanofibrous yarns [11, 12]. Instead of using the traditional needle as an outflow channel and high static electricity as a power source, blown bubble-spinning utilizes high velocity air-flow with certain temperature to stretch the jets from polymer bubbles for the final generation of nanofibers. Similar to the principles of two well-known technologies, melt-blowing [13] and solution blowing [14], blown bubble-spinning makes full use of air drawing force to overcome the solution surface tension and it is easy to adjust the experimental parameters to control the structure of nanofibers.

The goal of this work is to study the influences of the air-flow parameters including air-flow temperature and velocity on the morphology of nanofibers and nanofibrous yarns produced by blown bubble-spinning, so as to explore the feasibility of scaling up of this method.

Experimental

The Nylon6/66 ($C_{18}H_{37}N_3O_5$, $M_w = 375.5$ kDa) was purchased from Sigma, USA. The spun solutions were prepared by dissolving nylon6/66 at the concentration of 12% in formic acid (88% v/v, Sinopharm Chemical Reagent Co., Ltd, China) under slight stirring for 4 hours.

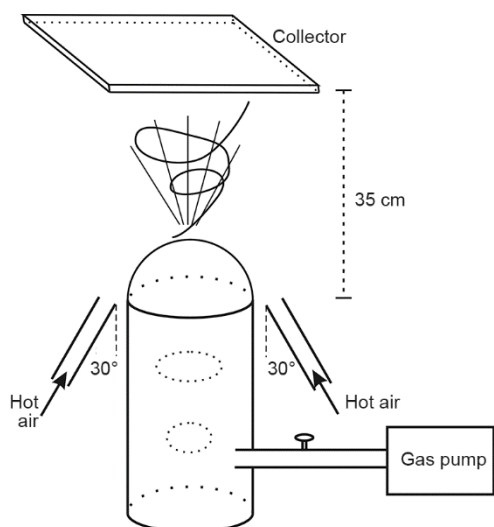


Figure 1. The schematic of the blown bubble-spinning

of the products obtained were measured from randomly collected SEM images using the IMAGE J software and expressed as mean \pm standard deviation (SD).

As previously described by our group [11, 12], the experimental setup of the blown bubble-spinning is shown in fig. 1. Compressed gas was released inside the solution to generate continuous bubbles at the orifice. Meanwhile, the blowing hot air in the form of two streams, that shaped a 60° angle, pulled the droplets of the bubble upwards rapidly and steadily, then nanofibers were obtained on the above collector. The diameter of orifice was 10 mm and the die-to-collector distance was 35 cm. This procedure was repeated by varying the air-flow temperature from 40°C to 200°C and air-flow velocity ranged from 10 m/s to 50 m/s, while holding all other operating parameters constant.

The morphology of nanofibers was observed using an SEM (Hitachi S-4800, Japan) at 20°C , 60% RH. Samples were mounted on a copper plate and sputter-coated with gold layer 20-30 nm thick prior to imaging. The diameters

Results and discussion

Air-flow temperature played a key role in the whole spinning process. It not only affected the initial acceleration and elongation of the jets, but also influenced the fiber curing and forming process. As could be seen from fig. 2 which showed the SEM of PA6/66 nanofibers and yarns under different air-flow temperatures, when the temperature of the air-flow was changed from 40°C (less than the glass transition temperature of nylon) to 80°C , the products became initially from a large number of irregular droplet agglomeration to a broad band, res-

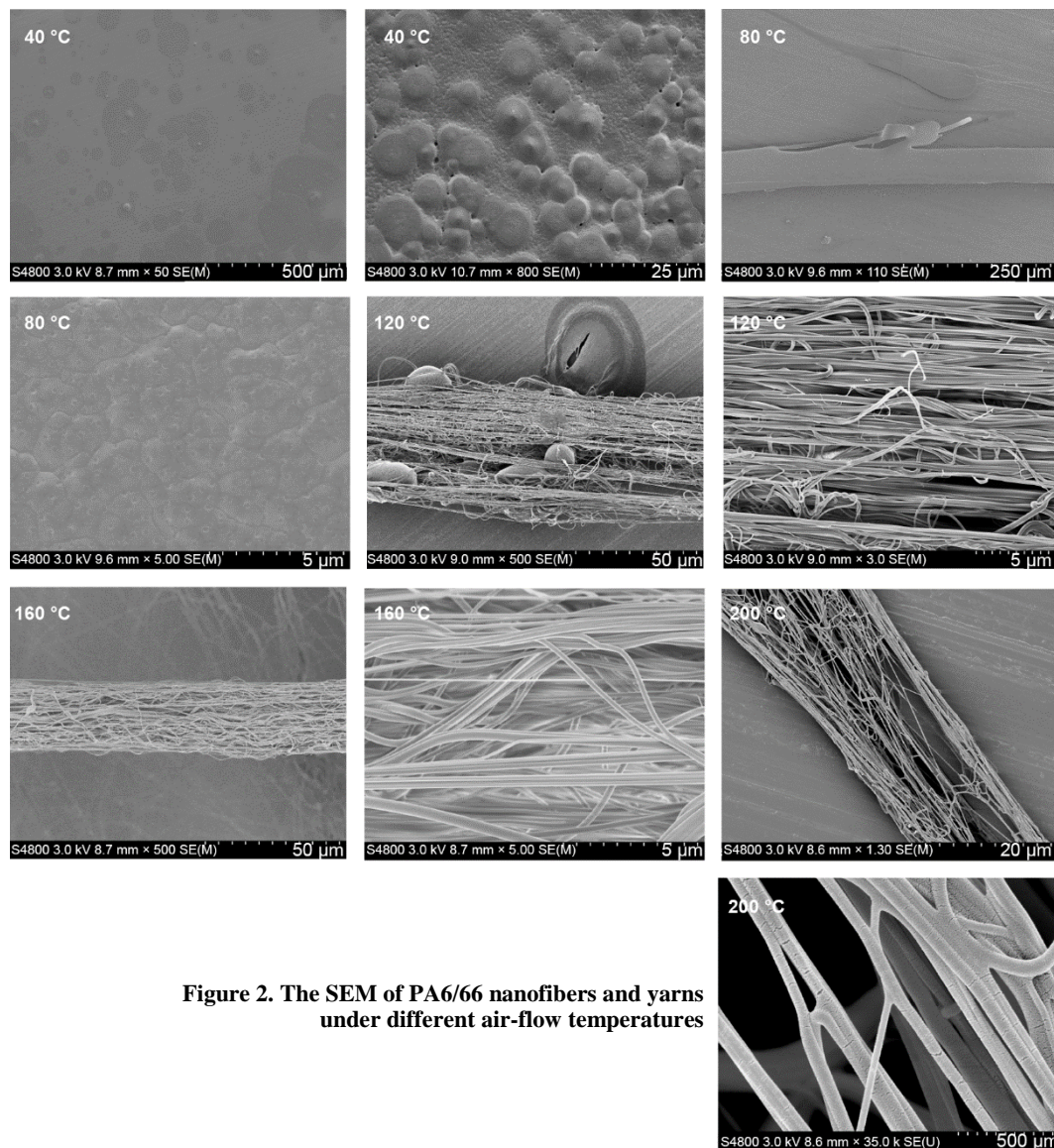


Figure 2. The SEM of PA6/66 nanofibers and yarns under different air-flow temperatures

pectively, revealing poor ability to fiber formation. With the temperature increasing to 120 °C, the morphology of products further changed into the fibrous bundle with bead-on-string structure. When the air temperature arrived at 160 °C, excellent fibrous yarns with closely arranged nanofibers were obtained. Furthermore, separation between nanofibers and voids on nanofibers occurred as the temperature was raised to 200 °C. According to the diameter statistics of PA6/66 nanofibers and yarns from fig. 3, it was clearly seen that the diameter of both nanofibers and yarns decreased with the increase of air-flow temperature. In addition, the minimum diameter of nanofibers was only over 100 nm, and the diameter of fiber bundle was about 30 μm.

According to [15], polymer bubbles own an interesting property that the surface tension σ of a polymer bubble geometrically depends upon its size and the pressure difference:

$$\sigma = \frac{1}{4} r (P_i - P_o) \quad (1)$$

where r is the radius of a bubble, P_i and P_o are the air pressures inside and outside the bubble, respectively.

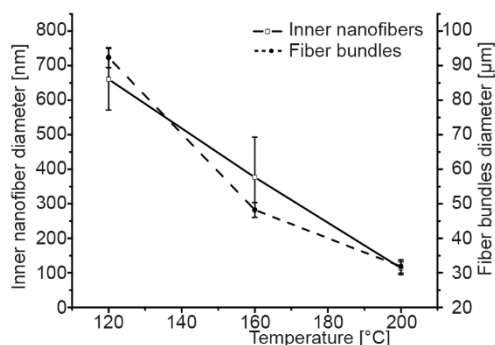


Figure 3. The diameter statistics of PA6/66 nanofibers and yarns by blown bubble-spinning under different air-flow temperatures

According to the ideal gas state equation, it is easy to get the following equation:

$$\sigma = \frac{1}{4} r R (T_i \rho_i - T_o \rho_o) \quad (2)$$

where R is gas constant, T_i , T_o , ρ_i , and ρ_o are inside and outside temperature and density of bubbles, respectively.

Based on eq. (2), it is obvious that there is inverse proportional relationship between surface tension and outside temperature of bubbles, namely, the diameter will go down because surface tension will reduce as increasing the outside temperature, which leads to less resistance and greater acceleration.

From the aspect of energy and heat exchange, higher temperature will result in more active movement of polymer macromolecules, which weakens the inner entanglement of macromolecules and promotes the ease to stretch jets. However, excessive heat causes fast evaporation of solvent and solidification of fibers, leading to cracks and loose nanofibers due to overstretch and instability.

As shown in fig. 4, it could be observed that the fiber morphology changed from irregular agglomeration with little fiber formation to a ball-like aggregate with a few fibers when the air-flow velocity increased from 10 m/s to 20 m/s. As the air-flow velocity increased, the nanofibers became smooth and the diameter decreased sharply, but a large number of particles were appeared on the rough nanofibers when velocity reached 50 m/s, which seriously affected the fiber morphology. According to the diameter statistics in fig. 5, the diameter of nanofibers and yarns decreased with the increase of air-flow velocity.

The reasons for the previous phenomena were explained by 1-D mass equation:

$$\rho u A = \rho \pi r^2 u = Q \quad (3)$$

where ρ is the jet density, u – the jet velocity, A – the jet cross area, r – the jet radius, and Q – the flow rate of jet.

Equation (3) indicates that finer nanofibers can be fabricated at higher air-flow rates, given that the flows are steady and solvent evaporation is negligible, which shows the same law

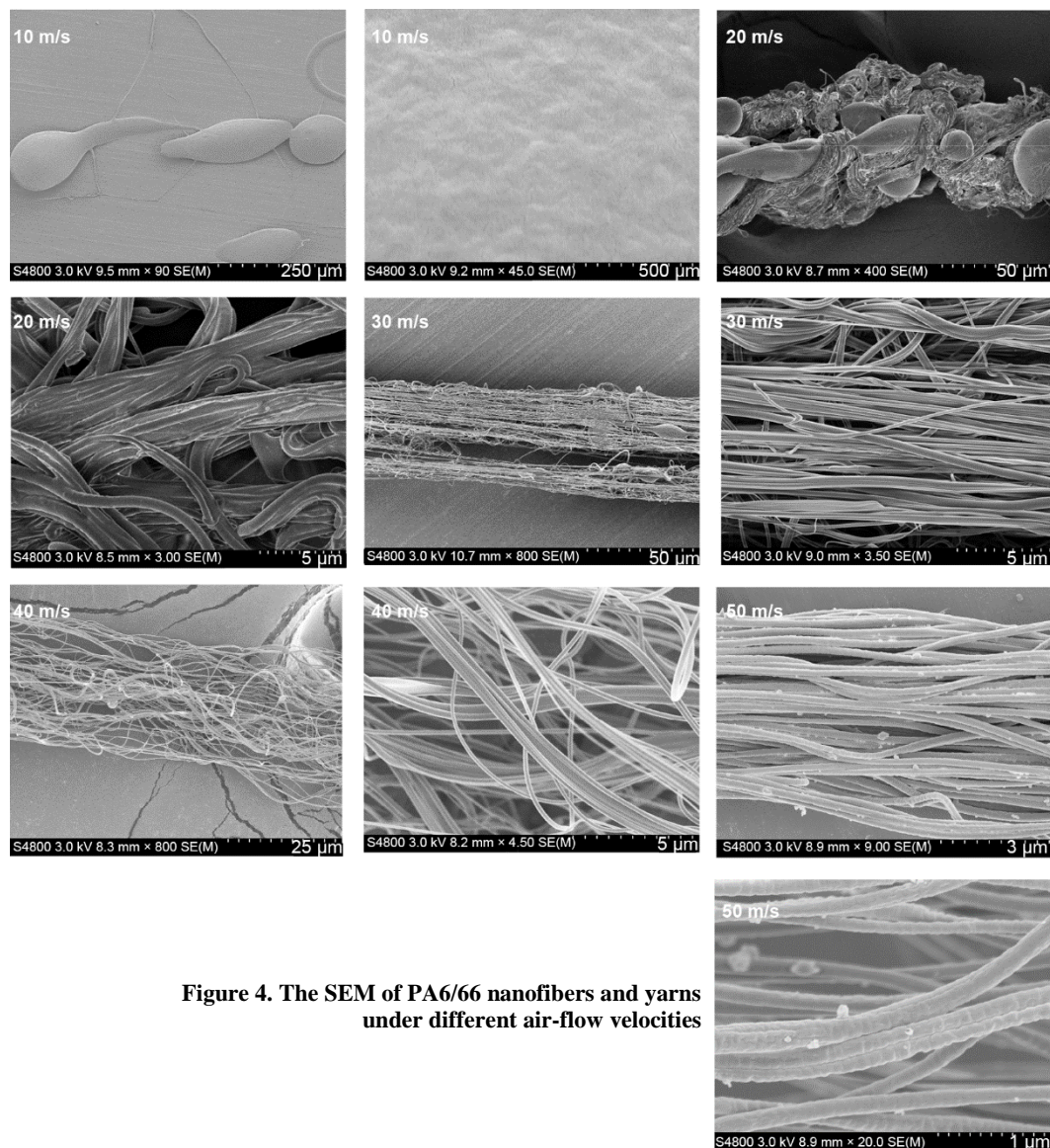


Figure 4. The SEM of PA6/66 nanofibers and yarns under different air-flow velocities

of physics in electrospinning [16-28]. Besides, air-flow velocity represents the energy applied to overcome the drag force for attenuating the fibers.

Conclusion

Blown bubble-spinning provides a novel and effective way for fabrication of nanofibrous yarns by introducing a high velocity air-flow with certain temperature acting on the ruptured jets from polymer bubbles. Increasing air-flow temperature and velocity accelerates the fineness of nanofibers and attributes to the interaction of multiple spinning jets, forming the nanofibrous yarns in one-step process.

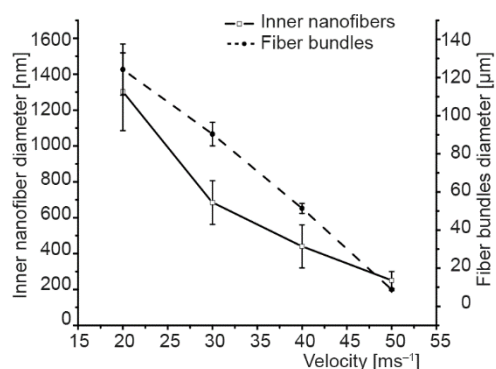


Figure 5. The diameter statistics of PA6/66 nanofibers and yarns by blown bubble-spinning under different air-flow velocities

Acknowledgment

The work is supported by the Natural Science Basic Research Plan in Shaanxi Province of China (Program No. 2017JQ5054), the Doctoral Scientific Research Foundation of Xi'an Polytechnic University (BS15015), Thousand Talents Program of Shaanxi Province, Sanqin Scholar Foundation of Shaanxi Province, National Natural Science Foundation of China (Grant No. 51603163) and Priority Academic Program Development of Jiangsu Higher Education Institutions (PAPD).

References

- [1] He, J. H., et al., Review on Fiber Morphology Obtained by the Bubble Electrospinning and Blown Bubble Spinning, *Thermal Science*, 16 (2012), 5, pp. 1263-1279
- [2] Rabiei, N., Haghghat Kish, M., Extraction of Nanofibers from Polymer Blends: A Brief Review, *Polymers for Advanced Technologies*, 30 (2019), 4, pp. 813-822
- [3] Liu, P., He, J. H., Geometric Potential: An Explanation of Nanofiber's Wettability, *Thermal Science*, 22 (2018), 1, pp. 237-243
- [4] Tian, D., et al., Self-Assembly of Macromolecules in a Long and Narrow Tube, *Thermal Science*, 22 (2018), 4, pp. 1659-1664
- [5] Tian, D., et al., Macromolecule Orientation in Nanofibers, *Nanomaterials*, 8 (2018), 11, ID 918
- [6] Xue, J., et al., Electrospinning and Electrospun Nanofibers: Methods, Materials, and Applications, *Chemical reviews*, 1119 (2019), 8, pp. 5298-5415
- [7] Ali, U., et al., Direct Electrospinning of Highly Twisted, Continuous Nanofiber Yarns, *Journal of the Textile Institute*, 103 (2012), 1, pp. 80-88
- [8] Yousefzadeh, M., et al., Producing Continuous Twisted Yarn from Well-Aligned Nanofibers by Water Vortex, *Polymer Engineering & Science*, 51 (2011), 2, pp. 323-329
- [9] Goktepe, F., Mulayim, B. B., Long Path Towards to Success in Electrospun Nanofiber Yarn Production Since 1930's: A Critical Review, *Autex Research Journal*, 18 (2018), 2, pp. 87-109
- [10] Rawlins, J., Kang, J., Fine Liquid Blowing: A High Reynolds Number, High Production Rate Nanofiber Manufacturing Technique, *Journal of Applied Polymer Science*, 136 (2019), 17, ID 47384
- [11] Dou, H., et al., Blown Bubble-Spinning for Fabrication of Superfine Fibers, *Thermal Science*, 16 (2012), 5, pp. 1465-1466
- [12] Dou, H., et al., Effect of Solution Concentrations on the Morphology of Nylon6/66 Nanofibrous Yarns by Blown Bubble-Spinning, *Matéria (Rio de Janeiro)*, 19 (2014), 4, pp. 358-362
- [13] Chen, T., et al., Numerical Computation of the Fiber Diameter of Melt Blown Nonwovens Produced by the Inset Die, *Journal of Applied Polymer Science*, 111 (2009), 4, pp. 1775-1779
- [14] Tan, N. P., et al., Solution Blow Spinning (SBS) Nanofibers for Composite Air Filter Masks, *ACS Applied Nano Materials*, 2 (2019), 4, pp. 2475-2483
- [15] He, J. H., Effect of Temperature on Surface Tension of a Bubble and Hierarchical Ruptured Bubbles for Nanofiber Fabrication, *Thermal Science*, 16 (2012), 1, pp. 327-330

- [16] Tian, D., He, J. H., Macromolecular Electrospinning: Basic Concept & Preliminary Experiment, *Results in Physics*, 11 (2018), Dec., pp. 740-742
- [17] Yu, D. N., et al., Snail-Based Nanofibers, *Materials Letters*, 220 (2018), 1, pp. 5-7
- [18] Li, X. X., He, J. H., Nanoscale Adhesion and Attachment Oscillation Under the Geometric Potential, Part 1: The Formation Mechanism of Nanofiber Membrane in the Electrospinning, *Results in Physics*, 12 (2019), Mar., pp. 1405-1410
- [19] Liu, Y. Q., et al., Nanoscale Multi-Phase Flow and Its Application to Control Nanofiber Diameter, *Thermal Science*, 22 (2018), 1, pp. 43-46
- [20] Liu, Z., et al., A Mathematical Model for the Formation of Beaded Fibers in Electrospinning, *Thermal Science*, 19 (2015), 4, pp. 1151-1154
- [21] Li, X. X., et al., The Effect of Sonic Vibration on Electrospun Fiber Mats, *Journal of Low Frequency Noise, Vibration and Active Control*, 38 (2019), 3-4, pp. 1246-1251
- [22] Liu, L. G., et al., Electrospun Polysulfone/Poly (Lactic Acid) Nanoporous Fibrous Mats for Oil Removal from Water, *Adsorption Science & Technology*, 37 (2019), 5-6, pp. 438-450
- [23] Li, Y., et al., Fabrication and Characterization of ZrO₂ Nanofibers by Critical Bubble Electrospinning for High-Temperature-Resistant Adsorption and Separation, *Adsorption Science & Technology*, 37 (2019), 5-6, pp. 425-437
- [24] He, J. H., et al. Variational Iteration Method for Bratu-Like Equation Arising in Electrospinning, *Carbohydrate Polymers*, 105 (2014), May, pp. 229-230
- [25] Chen, R. X., et al., Numerical Approach to Controlling a Moving Jet's Vibration in an Electrospinning System: An Auxiliary Electrode and Uniform Electric Field, *Journal of Low Frequency Noise, Vibration and Active Control*, 38 (2019), 3-4, pp. 1687-1698
- [26] Zhao, J. H., et al., Needle's Vibration in Needle-Disk Electrospinning Process: Theoretical Model and Experimental Verification, *Journal of Low Frequency Noise, Vibration and Active Control*, 38 (2019), 3-4, pp. 1338-1344
- [27] Zhang, L., et al., Vibration of an Axially Moving Jet in a Dry Spinning Process, *Journal of Low Frequency Noise, Vibration and Active Control*, 38 (2019), 3-4, pp. 1125-1131
- [28] Zhou, C. J., et al., Silkworm-Based Silk Fibers by Electrospinning, *Results in Physics*, 15 (2019), Dec., 102646